ELSEVIER

Journal of Molecular Catalysis A: Chemical 182–183 (2002) 81–88

JOURNAL OF MOLECULAR CATALYSIS A: CHEMICAL

www.elsevier.com/locate/molcata

Non-hydrolytic sol–gel routes based on alkyl halide elimination: toward better mixed oxide catalysts and new supports Application to the preparation of a SiO_2–TiO_2 epoxidation catalyst

V. Lafond, P.H. Mutin*, A. Vioux

Université Montpellier II, Sciences et Techniques du Languedoc, case 007, Place E. Bataillon, F 34095 Montpellier Cedex 5, France

Received 5 July 2001; accepted 15 October 2001

Abstract

The first part of this article is a concise review on non-hydrolytic sol-gel routes based on alkyl halide elimination. The molecular chemistry founding these routes is presented, as well as examples of applications to the synthesis of oxides and mixed oxides that may be of interest as catalysts or supports. In the second part, the straightforward non-hydrolytic preparation of a SiO_2–TiO_2 catalyst (not involving supercritical drying) is reported. The resulting SiO_2–TiO_2 calcined xerogel was highly homogeneous and displayed a high BET surface area located mainly in the mesopore region. Preliminary tests in the epoxidation of cyclohexene by cumene by hydroperoxide indicated good selectivity and activity.

Keywords: Sol–gel; SiO_2–TiO_2; Non-hydrolytic condensation; Mixed oxide; Epoxidation

1. Introduction

The preparation of supports and heterogeneous catalysts by sol–gel processing has attracted increasing interest in recent years. Sol–gel processing allows the formation of oxides with controlled porosity and shape (coatings, fibers, powders, monoliths). It is particularly useful for the preparation of multicomponent oxides with a high degree of homogeneity [1–3]. Actually, the ability of sol–gel to form mixed M–O–M′ bonds (where M and M′ denote two different metal atoms) leads to high densities of acid sites, while providing the high surface area and pore volume desired for catalytic applications [4].

The conventional sol–gel routes are based on the hydroxylation and polycondensation of molecular precursors, leading to the formation of the oxide network. The hydroxylation is achieved either by varying the pH in aqueous solutions of inorganic salt precursors (chlorides, nitrates, etc.) or by hydrolyzing alkoxide precursors in an organic solvent. Owing to the moderate reactivity of silicon precursors toward hydrolysis, these "hydrolytic" routes are well suited to the preparation of silica. On the other hand, metal and transition metal precursors are much more reactive, which may lead for instance to precipitates or to inhomogeneous multicomponent oxides. To overcome these problems, it is possible either to use inhibitors, such as inorganic acids or multidentate ligands (carboxylic acids, β-diketones, etc.), to tune the reactivity of the metal alkoxides [5–8] or to prehydrolyze the precursor having the lowest condensation rate [7,9]. Another possibility is to use non-hydrolytic sol–gel routes, based on different precursors, experimental conditions, and reaction mechanisms [10].

* Corresponding author. Fax: +33-4-67-14-38-52.
E-mail address: mutin@univ-montp2.fr (P.H. Mutin).

1381-1169/02/$ – see front matter
PII: S1381-1169(01)00487-3

In the past 10 years, several non-hydrolytic syntheses of oxides and mixed oxides have been investigated, involving for instance condensation with elimination of ester [11,12] or alkyl halide [13–31]. In this paper, we will focus on non-hydrolytic sol–gel routes based on the elimination of alkyl chloride, which have been developed in our group in the last 10 years.

Despite the excellent potentialities of non-hydrolytic routes for the preparation of highly homogeneous multicomponent oxides, there have been very few studies on the catalytic performances of multicomponent oxides derived from these routes [31].

A few years ago we published the non-hydrolytic sol–gel synthesis of homogeneous SiO_2–TiO_2 mixed oxides [18]. Here we investigated the application of these materials as epoxidation catalysts, prompted by the considerable interest of such mixed oxides in the epoxidation of alkenes [32]. Indeed, the activity and selectivity of SiO_2–TiO_2 catalysts strongly depend on their degree of homogeneity [33]. Amorphous SiO_2–TiO_2 catalysts have been prepared by conventional sol–gel process, using titanium alkoxides modified by chelating ligands [34], prehydrolysis of the silicon alkoxide precursor [9,35] or a mixed diethoxysiloxane–ethyltitanate precursor [36] to maximize the formation of Si–O–Ti linkages. More recently, the thermolysis of the complex $Ti[OSi(OtBu)_3]_4$ was used to prepare an active SiO_2–TiO_2 epoxidation catalyst [37].

In this paper, we first briefly present the molecular chemistry founding non-hydrolytic routes, and review their applications to the synthesis of oxides and mixed oxides, which could be useful as catalyst supports or as catalysts. Then, we report the preparation of a SiO_2–TiO_2 catalyst, and promising preliminary tests in the epoxidation of cyclohexene by cumene hydroperoxide.

2. Background

2.1. Molecular chemistry

The non-hydrolytic condensation between metal chlorides and metal alkoxides with elimination of alkyl chloride provides an attractive method to form the oxide network. This reaction (Eq. (1)) involves the nucleophilic cleavage of O–R bonds and is, therefore, influenced by the electronic effects on the carbon center. In the case of metals and transition metals, condensation occurs at temperatures ranging from room temperature to about 100 °C. Silicon is less reactive, and tertiary alkyl or benzylic R groups are needed. Otherwise, Lewis acids, such as iron or aluminum chloride, are required to catalyze the condensation.

$$\text{M–Cl} + \text{M–OR} \rightarrow \text{M–O–M} + \text{R–Cl} \quad (1)$$

The alkoxy groups may be produced in situ by the etherolysis (Eq. (2)) or the alcoholysis (Eq. (3)) of metal chlorides, which is particularly interesting if the alkoxide is expensive or is not commercially available.

$$\text{M–Cl} + \text{ROR} \rightarrow \text{M–OR} + \text{RCl} \quad (2)$$

$$\text{M–Cl} + \text{ROH} \rightarrow \text{M–OR} + \text{HCl} \quad (3)$$

This led us to propose three different non-hydrolytic routes to oxides and mixed oxides, based on the condensation between metal or silicon chlorides with either alkoxides, ethers or alcohols as oxygen donors. Note that the redistribution of OR and Cl ligands (Eq. (4)) usually takes place at room temperature. Thus, the true precursors in these routes are chloroalkoxide species.

$$\text{M–Cl} + \text{M}'\text{–OR} \rightarrow \text{M–OR} + \text{M}'\text{–Cl} \quad (4)$$

The kinetics of non-hydrolytic sol–gel appears quite complicated, and depends on the nature of the element, the nature of the oxygen donor, and the composition of the initial chloroalkoxide mixture [38].

2.2. Application to the synthesis of oxides and mixed oxides

The alkoxide, ether, and alcohol routes have been used for the preparation of oxides and mixed oxides with different structures and textures, which well illustrates the versatility of these methods. In addition, oxides without hydroxyl surface groups as well as non-hydrated oxides can be obtained using these non-hydrolytic routes.

2.2.1. Oxides

Non-hydrolytic sol–gel routes have been used for the preparation of SiO_2 [13,22,39], Al_2O_3 [16,26,27,40], TiO_2 [19,25,38], ZrO_2 [17,28], WO_3 [17,28], Nb_2O_5 [17] and Fe_2O_3 [17]. Moreover,

non-hydrolytic condensation with elimination of alkyl chloride was used for the processing of tantalum oxide films by atomic layer deposition (ALD) and chemical vapor deposition (CVD) from $TaCl_5$ and $Ta(OEt)_5$ [41]. Non-hydrolytic condensations could also be involved in the preparation of mesoporous oxides and mixed oxides (TiO_2, ZrO_2, Nb_2O_5, Ta_2O_5, Al_2O_3, SnO_2, HfO_2, WO_3, etc.) using metal chlorides and alcohols in the presence of amphiphilic block copolymers as structure-directing agents [42,43].

In the case of silica, it was shown that non-porous, mesoporous or predominantly microporous silicas can be obtained depending on the nature of the oxygen donor and of the catalyst [22].

Conventional sol–gel processing of alumina leads to pseudo-boehmites that usually crystallize to γ-Al_2O_3 below 500 °C. Non-hydrolytic alumina gels obtained using the alkoxide route led after calcination to non-hydrated aluminas, that remained amorphous after heating for 5 h at 750 °C, while keeping specific surface areas higher than 300 m^2/g [16]. Solid-state ^{27}Al NMR spectra of these aluminas indicated a large amount of pentacoordinated aluminum sites, which may be regarded as structural defects giving an explanation for the delayed crystallization. Moreover, pentacoordinated aluminum sites were evidenced in the initial solutions, indicating that the presence of these sites in the gels and in the amorphous aluminas might be directly related to the structure of the chloroalkoxide precursors [40]. Alumina foams with exceptionally high porosity and a cellular structure retained up to 1500 °C were generated by the heat treatment of crystals of the aluminum chloride isopropyl ether complex $AlCl_3 \cdot {}^{i}Pr_2O$, leading to the elimination of isopropyl chloride [26,27].

In the case of titania, non-hydrolytic sol–gel methods allow the formation of a particular crystalline structure by varying the nature of the oxygen donor (ether or alcohol), as do conventional sol–gel methods by controlling the hydrolysis conditions. Thus, the reaction of diethyl ether with $TiCl_4$ at 110 °C affords anatase, which begins to convert into rutile only around 950 °C. On the other hand, the reaction of $TiCl_4$ with ethanol leads to rutile as early as 110 °C, whereas the reaction of tertiobutanol at 110 °C leads to the formation of brookite, which is a quite uncommon phase in synthetic products [19]. Quite recently, anatase nanocrystals with no surface hydroxyl groups have been prepared at 300 °C in heptadecane using the alkoxide route in the presence of a passivating agent (trioctylphosphine oxide) [25].

2.2.2. Mixed oxides

One of the main asset of our non-hydrolytic sol–gel routes is that they allow a very simple preparation of mixed oxides. Many systems have been investigated, including SiO_2–ZrO_2 [18], SiO_2–TiO_2 [18,23], SiO_2–Al_2O_3 [23,40,44,45], TiO_2–Al_2O_3 [20,30], TiO_2–ZrO_2 [21,29], V_2O_5–Nb_2O_5 [31], V_2O_5–SiO_2–Nb_2O_5 [31], ZrO_2–WO_3 [28] and NASICON ($Na_3Zr_2Si_2PO_{12}$) [46]. Non-hydrolytic condensation was also used to deposit aluminosilicate films on graphite surfaces or to prepare V–Ti–Si catalysts by surface modification of a silica support with $VOCl_3$ and $Ti(O^{i}Pr)_4$ [47] or to grow Li_2O–Nb_2O_5 films on MgO or $LiTaO_3$ substrates [48].

Owing to the redistribution reactions, the chloride and alkoxide groups are bonded to the different metal centers. Thus, both heterocondensation and homocondensation may occur, leading to a mixture of M–O–M′, M–O–M, and M′–O–M′ bridges. It is assumed that non-hydrolytic routes lead to better control over the molecular level homogeneity and composition than hydrolytic routes. This could be due to a leveling of the heterocondensation and homocondensation rates, related to the mechanism of these reactions and the use of non-aqueous media, which allows the formation of a high level of mixed M–O–M′ bridges. For instance, although the non-hydrolytic condensation around silicon atoms is quite slow in the absence of a zirconium, it is efficiently catalyzed by the Lewis acid zirconium species. As a result, SiO_2–ZrO_2 mixed oxides prepared by the alkoxide or the ether route appeared highly homogeneous: they remained amorphous after calcination at 600 °C for 5 h, and ^{29}Si NMR spectroscopy clearly showed the presence of numerous Si–O–Zr bridges in these glasses [18].

The proof of the homogeneity of a SiO_2–TiO_2 sample containing 5 mol% TiO_2 was provided by the direct crystallization at 900 °C of single phase cristobalite. The cell parameters were slightly higher than those of pure silica cristobalite, showing the formation of a solid solution of titania in silica, with Ti^{4+} ions substituting Si^{4+} ions at random. On the other hand, precipitation of anatase was observed for samples with a high Ti content (20–50 mol% TiO_2),

which are outside the stable glass region. However, FTIR indicated the presence of Si–O–Ti bonding, and the anatase to rutile transformation was not observed, even after 2 h at 1300 °C [18].

In the TiO_2–ZrO_2 system, the direct crystallization of $ZrTiO_4$ below 700 °C, without the intermediate formation of TiO_2 or ZrO_2, may be ascribed to the good homogeneity of the non-hydrolytic gels [21]. Quite recently, X-ray absorption studies (EXAFS) clearly indicated the presence of Zr–O–Ti linkages in a $ZrTiO_4$ gel prepared by the ether route [29].

Interesting results were observed in the TiO_2–Al_2O_3 system. The definite compound Al_2TiO_5 is known to be metastable below ∼1180 °C, the stable phases being TiO_2 (rutile) and α-Al_2O_3 (corundum). Samples with a Al/Ti ratio of 2, arising from the non-hydrolytic alkoxide and ether routes, have been found to crystallize above 600 °C as β-Al_2TiO_5. This result may be ascribed to the excellent molecular scale homogeneity of the non-hydrolytic gels that favors the direct crystallization of the metastable Al_2TiO_5 phase, rather than the phase separation to the stable rutile and corundum phases, which would require long-range metal-ion diffusion [20]. 0.6 TiO_2–0.4 Al_2O_3 catalytic supports have been prepared by hydrolytic and non-hydrolytic processes [30]. The authors found that the texture, the distribution of acid sites, and the crystallization behavior were influenced by the synthesis method.

Interestingly, in the ZrO_2–WO_3 system, non-hydrolytic sol–gel processing allowed the formation of a new metastable ZrW_2O_8 polymorph, structurally related to trigonal $ZrMo_2O_8$ [28].

$NbVO_5$ micrometric crystallites have been recently obtained from $NbCl_5$ and $VO(O^iPr)_3$. These crystallites and an amorphous V–SiO_2–Nb mixed oxide showed interesting performances as catalysts in the oxidative dehydrogenation of propane [31].

3. Experimental

All manipulations were performed under an argon atmosphere using standard Schlenck techniques and an inflatable glovebox. Elemental analyses were performed by the "Service Central d'Analyse du CNRS" at Vernaison, France. Si and Ti content were determined by inductively coupled plasma (ICP) from aqueous solutions. X-ray powder diffraction was used with Cu Kα radiation to identify the oxide phase after thermal treatment (Siefert MZ IV diffractometer). The IR spectra of the solids in KBr pellets (2.6 mg xerogel powder in 165 mg KBr) were recorded on a Perkin Elmer 1600 series FTIR spectrophotometer. N_2 adsorption–desorption experiments were performed at 77 K using a Micromeritics ASAP 2010. Thermal analysis was performed in dry air, at a heating rate of 10 K min^{-1}, on a Netzch STA 409 thermobalance. Epoxidation reactions were monitored by gas chromatography (GC) (FID) using a Hewlett-Packard chromatograph, an HP-5 (DB-5 type) diphenyl (5%)–dimethylsiloxane (95%) column (30 m × 0.25 mm × 0.25 μm), nitrogen as carrier gas (11 psi), injector temperature 190 °C, detector temperature 260 °C. Nonane was used as an internal standard. Assignment of products was made by comparison with authentic samples analyzed under the same conditions.

$Si(O^iPr)_4$ was prepared according to the literature procedure [49]. $SiCl_4$ (Acros 99.8%) and $Ti(O^iPr)_4$ (Lancaster 97%) were distilled before use. Toluene (Prolabo normapure) was dried and degassed before use. Isopropanol (Carlo Erba 99.7%), cyclohexene (Lancaster 99%), nonane (Aldrich 99%), and cumyl hydroperoxyde (Lancaster, tech. 80%) were used as received.

3.1. Preparation of the catalysts

The SiO_2–TiO_2 mixed oxide was prepared according to the literature procedure [18]. $SiCl_4$ (6.87 g, 40.4 mmol), $Si(O^iPr)_4$ (8.74 g, 33.1 mmol) and $Ti(O^iPr)_4$ (2.10 g, 7.39 mmol) were added successively with a syringe into a Pyrex ampoule connected to a schlenck line. A limpid, colorless solution formed on shaking. The ampoule was then sealed and kept for 4 days at 110 °C in a oven. A yellow transparent monolithic solid was obtained, together with a limpid colorless liquid, which proved to be ^iPrCl (^{1}H-NMR ($CDCl_3$ δ ppm): 4.23(sept. 1H) 1.55 (d 6H)). The sealed tube was opened under argon in a glovebox, the solid filtered off, washed three times with dry CH_2Cl_2 and dried under vacuum at 110 °C for 6 h, leading after crushing in a mortar to a light orange xerogel powder.

Calcination in dry air at 550 °C for 2 h led to a white powder (weight loss 17.7%).

Anal. Calc.: Ti, 7.13 wt.%; Si, 41.12 wt.%. Found: Ti, 7.0 wt.%; Si, 39.4 wt.%.

For comparison, Shell epoxidation catalyst [50] was prepared by surface modification of silica (Degussa Aerosil 200) with $Ti(O^iPr)_4$ modified by acacH and calcined in dry air at 600 °C as described in the literature [37].

Found: Ti, 0.9 wt.%.

3.2. Epoxidation procedure

Fifty milligrams of catalyst was added to a 50 ml two-necked round-bottom flask fitted with a condenser that had previously been evacuated and filled with argon three times. Toluene (Prolabo normapure, dried and degassed) (5 ml), cyclohexene (2.5 ml, 24.7 mmol), and nonane (0.25 ml) were added by syringe through a septum. After equilibration for 10 min at the reaction temperature (65 °C), cumyl hydroperoxyde (0.92 ml) was added by syringe to the stirred solution. Aliquots (ca. 0.25 ml) were removed from the reaction mixture by syringe, filtered and analyzed by GC.

4. Results and discussion

4.1. Preparation and characterization of the mixed oxide

A SiO_2–TiO_2 mixed oxide with a nominal TiO_2 content of 10 mol% was prepared by the alkoxide route, according to the idealized equation [18]:

$$5.5\,SiCl_4 + 4.5\,Si(O^iPr)_4 + 1\,Ti(O^iPr)_4 \rightarrow 10\,SiO_2 \cdot TiO_2 + 22\,{}^iPrCl$$

The only byproduct detected was ^iPrCl, indicating that gelation originated from non-hydrolytic condensation. The oxide obtained after calcination at 550 °C for 2 h was amorphous, according to X-ray diffraction. Elemental analysis showed a TiO_2 content of 9.4 mol% (7.0 wt.%), in good agreement with the expected one (9.1 mol%).

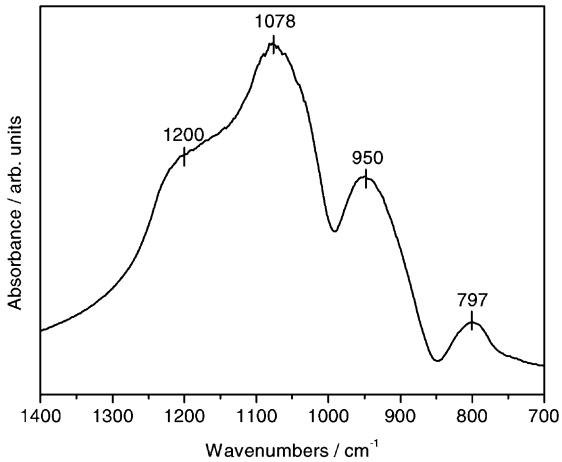

Fig. 1. FTIR spectrum of the calcined SiO_2–TiO_2 mixed oxide.

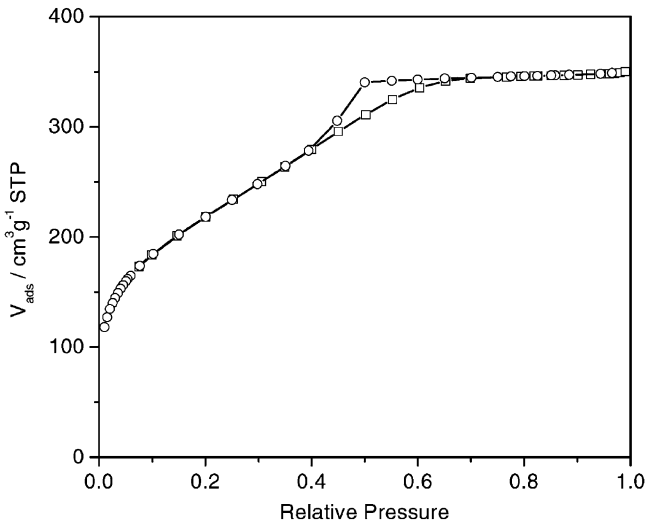

Fig. 2. N_2 physisorption isotherms (77 K) on the calcined SiO_2–TiO_2 mixed oxide. (□) Adsorption; (○) desorption.

The FTIR spectrum of our sample in the 1400–700 cm^{-1} range (Fig. 1) exhibited three broad bands typical of silica at 1200, 1078 cm^{-1} (TO and LO modes of the asymmetric Si–O–Si stretching vibration), and at 797 cm^{-1} (symmetric Si–O–Si stretching vibration) [2]. In addition, an intense band is observed at 950 cm^{-1}. This band has been ascribed to a vibration involving SiO_4 tetrahedra bonded to a four-fold coordinated titanium atom [9,18,34,51]. The high intensity of this band in our material is in favor of a large amount of Si–O–Ti linkages.

The N_2 adsorption–desorption isotherm of the SiO_2–TiO_2 mixed oxide (Fig. 2) was of type IV, according to the BDDT classification [52]. The specific surface area determined by the BET method [53] was $S_{BET} = 780\,m^2\,g^{-1}$. The total pore volume at $P/P_0 = 0.99$ was $V_p = 0.54\,cm^3\,g^{-1}$, which gave a mean pore diameter $D_p = 4V_p/S_{BET} = 2.8$ nm. According to the *t*-plot analysis [54] in the 3.5–5 Å range (Harkins and Jura standard isotherm) [55], the micropore volume was quite low ($0.01\,cm^3\,g^{-1}$). The pore volume and the specific surface area of mesopores in the 2–50 nm range (determined by the BJH method [56] from the desorption branch) were $V_{meso} = 0.37\,cm^3\,g^{-1}$ and $S_{meso} = 480\,m^2\,g^{-1}$. Comparison of these values with S_{BET} and V_p suggests the presence of significant microporosity. The BJH pore size distribution indicated the presence in our material of pores with diameter lower than 4 nm.

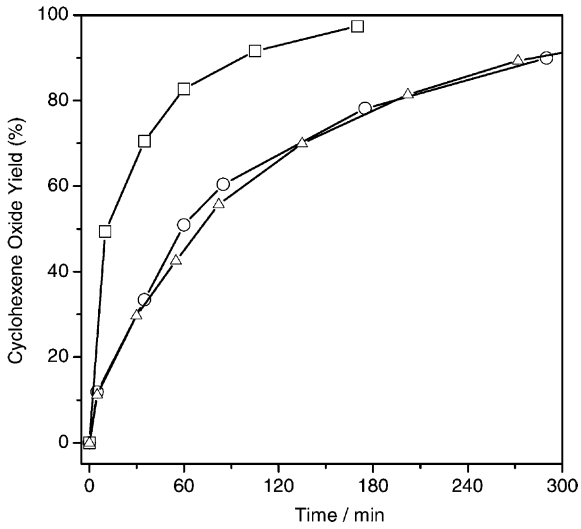

Fig. 3. Epoxidation of cyclohexene at 338 K with CHP catalyzed by calcined SiO_2–TiO_2 non-hydrolytic mixed oxide (□), the corresponding uncalcined xerogel (△) and the Shell catalyst (○).

4.2. Epoxidation of cyclohexene

Our non-hydrolytic SiO_2–TiO_2 mixed oxide was tested in the epoxidation of cyclohexene with cumyl hydroperoxide (CHP) at 65 °C. We found that this solid was a highly active and selective catalyst for this reaction. After 2 h at 65 °C, the yield of cyclohexene oxide (relative to CHP) was higher than 90% (Fig. 3). In another experiment, we showed that the reaction

Table 1
Results obtained for the epoxidation of cyclohexene with different SiO_2–TiO_2 mixed oxide catalysts and the Shell catalyst

Catalyst (wt.% Ti) (mg)	Ti (mmol)	Cyclohexene (mmol)	CHP (mmol)	*T* (°C)	Epoxide (%)[a]	TON[b]	Initial rate[c]
SiO_2–TiO_2 (7.0) (50)[d]	0.0731	25	5	65	91	62	4.8
Shell (0.9) (50)[d]	0.0094	25	5	65	68	360	2.6
10LT (6.0) (100)[e]	0.125	77	13.4	60	87	93	6.0
20LT (12.0) (100)[e]	0.251	77	13.4	60	93	50	7.8
SiO_2–TiO_2 (15.0) (50)[f]	0.157	25	5	65	49	15.6	2.8

[a] Cyclohexene epoxide yield relative to CHP after 2 h.
[b] mol epoxide (mol Ti)$^{-1}$ (2 h reaction time).
[c] mmol epoxide min^{-1} (g cat)$^{-1}$ (after 5 min reaction time).
[d] This work.
[e] Data from Ref. [57].
[f] Data from Ref. [37].

stopped when the oxide was filtered off after 30 min, indicating that the catalysis is truly heterogeneous.

Interestingly, the xerogel (before calcination) displayed a significantly lower activity than the oxide (after calcination), whereas Baiker and coworkers [57] reported that their uncalcined aerogel samples was slightly more active than the calcined ones. Actually, our xerogel showed practically the same activity (on a weight basis) than the Shell catalyst (Fig. 3) Comparison of our non-hydrolytic mixed oxide with other SiO_2–TiO_2 mixed oxide catalysts [37,57] is given in Table 1. In the case of our calcined xerogel, both epoxide yield and initial rate appear nearly as good as those reported by Baiker and coworkers [57] for a calcined aerogel sample containing 6 wt.% Ti.

In addition, it must be noted that the preparation of our catalyst is quite straightforward, requiring only a simple drying procedure instead of semicontinuous extraction with supercritical CO_2 [57]. Additional work is needed to further improve these promising results. Much remains to be done, such as playing on the nature of the solvent, the Ti content, the non-hydrolytic route (ether or alcohol instead of alkoxide).

5. Conclusions

Non-hydrolytic sol–gel routes are valuable alternatives to conventional sol–gel routes, as shown here by the simple preparation of a SiO_2–TiO_2 mixed oxide, highly active epoxidation catalyst. These non-hydrolytic routes have many beneficial features, such as

- simple syntheses with easily available precursors;
- solvent-free (Si, Ti) or large choice of solvents,
- cheap chloride precursors (ether or alcohol routes);
- low-hydroxyl content or anhydrous oxides;
- excellent control over the molecular level homogeneity of multicomponent oxides.

Up to now there have been very few applications of non-hydrolytic routes in the field of catalysis. However, given their huge potential in the synthesis of oxides and mixed oxides, exploration of these new routes for the preparation of catalysts supports and catalysts should attract increasing attention in the coming years.

References

[1] R.K. Iler, The Chemistry of Silica, Wiley, New York, 1979.
[2] C.J. Brinker, G.W. Scherer, Sol–Gel Science: The Physics and Chemistry of Sol–Gel Processing, Academic Press, Boston, MA, 1990.
[3] U. Schubert, J. Chem. Soc., Dalton Trans. (1996) 3343.
[4] J.B. Miller, E.I. Ko, Catal. Today 35 (1997) 269.
[5] J.C. Debsikar, J. Non-Cryst. Solids 87 (1986) 343.
[6] C. Sanchez, J. Livage, M. Henry, F. Babonneau, J. Non-Cryst. Solids 100 (1988) 65.
[7] B.E. Yoldas, J. Mater. Sci. 21 (1986) 1086.
[8] E. Scolan, C. Sanchez, Chem. Mater. 10 (1998) 3217.
[9] M.F. Best, R.A. Condrate, J. Mater. Sci. Lett. 4 (1985) 994.
[10] A. Vioux, Chem. Mater. 9 (1997) 2292.
[11] M. Jansen, E. Guenther, Chem. Mater. 7 (1995) 2110.
[12] J. Caruso, M.J. Hampden-Smith, J. Sol–Gel Sci. Technol. 8 (1997) 35.
[13] R.J.P. Corriu, D. Leclercq, P. Lefevre, P.H. Mutin, A. Vioux, J. Non-Cryst. Solids 146 (1992) 301.
[14] R.J.P. Corriu, D. Leclercq, P. Lefèvre, P.H. Mutin, A. Vioux, J. Mater. Chem. 2 (1992) 673.
[15] R.J.P. Corriu, D. Leclercq, P. Lefèvre, P.H. Mutin, A. Vioux, Chem. Mater. 4 (1992) 961.
[16] S. Acosta, R.J.P. Corriu, D. Leclercq, P. Lefèvre, P.H. Mutin, A. Vioux, J. Non-Cryst. Solids 170 (1994) 234.
[17] P. Arnal, R.J.P. Corriu, D. Leclercq, P.H. Mutin, A. Vioux, Mater. Res. Soc. Symp. Proc. 346 (1994) 339.
[18] M. Andrianainarivelo, R. Corriu, D. Leclercq, P.H. Mutin, A. Vioux, J. Mater. Chem. 6 (1996) 1665.
[19] P. Arnal, R.J.P. Corriu, D. Leclercq, P.H. Mutin, A. Vioux, J. Mater. Chem. 6 (1996) 1925.
[20] M. Andrianainarivelo, R.J.P. Corriu, D. Leclercq, P.H. Mutin, A. Vioux, Chem. Mater. 9 (1997) 1098.
[21] M. Andrianainarivelo, R.J.P. Corriu, D. Leclercq, P.H. Mutin, A. Vioux, J. Mater. Chem. 7 (1997) 279.
[22] L. Bourget, R.J.P. Corriu, D. Leclercq, P.H. Mutin, A. Vioux, J. Non-Cryst. Solids 242 (1998) 81.
[23] J.N. Hay, H.M. Raval, J. Mater. Chem. 8 (1998) 1233.
[24] J.N. Hay, H.M. Raval, J. Sol–Gel Sci. Technol. 13 (1998) 109.
[25] T.J. Trentler, T.E. Denler, J.F. Bertone, A. Agrawal, V.L. Colvin, J. Am. Chem. Soc. 121 (1999) 1613.
[26] Y. de Hazan, G.E. Shter, Y. Cohen, C. Rottman, D. Avnir, G.S. Grader, J. Sol–Gel Sci. Technol. 14 (1999) 233.
[27] G.S. Grader, G.E. Shter, Y. de Hazan, J. Mater. Res. 14 (1999) 1485.
[28] A.P. Wilkinson, C. Lind, S. Pattanaik, Chem. Mater. 11 (1999) 101.
[29] J. Xu, C. Lind, A.P. Wilkinson, S. Pattanaik, Chem. Mater. 12 (2000) 3347.
[30] R. Linacero, M.L. Rojas-Cervantes, J.D.D. Lopez-Gonzalez, J. Mater. Sci. 35 (2000) 3269.
[31] F. Barbieri, D. Cauzzi, F. De Smet, M. Devillers, P. Moggi, G. Predieri, P. Ruiz, Catal. Today 61 (2000) 353.
[32] M. Dusi, T. Mallat, A. Baiker, Catal. Rev-Sci. Eng. 42 (2000) 213.

[33] R.J. Davis, Z.F. Liu, Chem. Mater. 9 (1997) 2311.
[34] D.C.M. Dutoit, M. Schneider, A. Baiker, J. Catal. 153 (1995) 165.
[35] M. Schraml-Marth, K.L. Walther, A. Wokaun, B.E. Handy, A. Baiker, J. Non-Cryst. Solids 143 (1992) 93.
[36] J.B. Miller, L.J.M. Athers, E.I. Ko, J. Catal. 5 (1994) 1759.
[37] M.P. Coles, C.G. Lugmair, K.W. Terry, T.D. Tilley, Chem. Mater. 12 (2000) 122.
[38] P. Arnal, R.J.P. Corriu, D. Leclercq, P.H. Mutin, A. Vioux, Chem. Mater. 9 (1997) 694.
[39] J.N. Hay, D. Porter, H.M. Raval, J. Mater. Chem. 10 (2000) 1811.
[40] S. Acosta, R.J.P. Corriu, D. Leclercq, P.H. Mutin, A. Vioux, J. Sol–Gel Sci. Technol. 2 (1994) 25.
[41] K. Kukli, M. Ritala, M. Leskelä, Chem. Mater. 12 (2000) 1914.
[42] P. Yang, D. Zhao, D.I. Margolese, B.F. Chmelka, G.D. Stucky, Chem. Mater. 11 (1999) 2813.
[43] W. Cheng, E. Baudrin, B. Dunn, J.I. Zink, J. Mater. Chem. 11 (2001) 92.
[44] S. Acosta, R.J.P. Corriu, D. Leclercq, P.H. Mutin, A. Vioux, Mater. Res. Soc. Symp. Proc. 346 (1994) 345.
[45] D. Janackovic, A. Orlovic, D. Skala, S. Drmanic, L.K. Kostic-Gvozdenovic, V. Jokanovic, D. Uskokovic, Nanostructured Mater. 12 (1999) 147.
[46] M.L. Di Vona, E. Traversa, S. Licoccia, Chem. Mater. 13 (2001) 141.
[47] L.G. Rice, S.L. Scott, Chem. Mater. 10 (1998) 620.
[48] R.H. Kim, H.H. Park, G.T. Joo, Appl. Surf. Sci. 169 (2001) 564.
[49] D.C. Bradley, D.A. Hill, J. Chem. Soc. (1963) 2101.
[50] F. Wattinema, H.P. Wulff, UK Patent 1 249 079 (1971) to Shell Oil.
[51] C.F. Smith, R.A. Condrate, W.E. Votava, Appl. Spectrosc. 29 (1975) 79.
[52] S. Brunauer, L.S. Deming, W.E. Deming, E. Teller, J. Am. Chem. Soc 62 (1940) 1723.
[53] S. Brunauer, P.H. Emmett, E.J. Teller, J. Am. Chem. Soc. 60 (1938) 309.
[54] B.C. Lippens, J.H. deBoer, J. Catal. 4 (1965) 319.
[55] W.D. Harkins, G. Jura, J. Chem. Phys. 11 (1943) 431.
[56] E.P. Barrett, L.S. Joyner, P.P. Halenda, J. Am. Chem. Soc. 73 (1951) 373.
[57] R. Hutter, T. Mallat, A. Baiker, J. Catal. 153 (1995) 177.